

# Presynaptic GABA<sub>A</sub> receptors enhance transmission and LTP induction at hippocampal mossy fiber synapses

Arnaud Ruiz<sup>1,2</sup>, Emilie Campanac<sup>1,4</sup>, Ricardo S Scott<sup>1,3,4</sup>, Dmitri A Rusakov<sup>1</sup> & Dimitri M Kullmann<sup>1</sup>

**Presynaptic GABA<sub>A</sub> receptors (GABA<sub>A</sub>Rs) occur at hippocampal mossy fiber synapses. Whether and how they modulate orthodromic signaling to postsynaptic targets is poorly understood. We found that an endogenous neurosteroid that is selective for high-affinity  $\delta$  subunit-containing GABA<sub>A</sub>Rs depolarized rat mossy fiber boutons, enhanced action potential-dependent Ca<sup>2+</sup> transients and facilitated glutamatergic transmission to pyramidal neurons. Conversely, blocking GABA<sub>A</sub>Rs hyperpolarized mossy fiber boutons, increased their input resistance, decreased spike width and attenuated action potential-dependent presynaptic Ca<sup>2+</sup> transients, indicating that a subset of presynaptic GABA receptors are tonically active. Blocking GABA<sub>A</sub>Rs also interfered with the induction of long-term potentiation at mossy fiber–CA3 synapses. Presynaptic GABA<sub>A</sub>Rs therefore facilitate information flow to the hippocampus both directly and by enhancing LTP.**

Presynaptic GABA<sub>A</sub>Rs exist in several areas of the CNS. In comparison with somatodendritic receptors, relatively little is known of their pharmacological properties and physiological roles. Although they mediate presynaptic inhibition of glutamate release from primary muscle afferents in the spinal cord, they have a facilitatory effect on neurotransmitter release in the brainstem and cerebellum<sup>1,2</sup>. Whether presynaptic receptors in the cerebral cortex enhance or depress neurotransmitter release is less clear. Mossy fibers in the hippocampal formation offer a well-defined and relatively accessible pathway for examining presynaptic GABA<sub>A</sub>Rs<sup>3</sup>. In immature rats, activation of such receptors is accompanied by an increase in the amplitude of the fiber volley evoked by axon stimulation<sup>4</sup>. Furthermore, application of the GABA<sub>A</sub> receptor agonist muscimol enhances glutamate release from isolated boutons onto acutely dissociated pyramidal neurons<sup>5</sup>. Although these observations suggest that presynaptic GABA<sub>A</sub>Rs facilitate orthodromic transmission, this remains to be shown in a more intact preparation.

It is also unclear whether presynaptic GABA<sub>A</sub>Rs in mossy fibers are active in the absence of evoked GABA release. Examination of mossy fiber excitability in response to electrical stimulation revealed bidirectional effects of the GABA<sub>A</sub> receptor antagonist SR95531 (gabazine) depending on [Cl<sup>-</sup>]<sub>i</sub> in individual granule cells<sup>3</sup>, arguing that the receptors can be tonically active. However, whole-terminal recordings from mossy fiber boutons have not detected an effect of blocking GABA<sub>A</sub>Rs on input resistance<sup>6</sup>. Although direct recordings have confirmed that presynaptic GABA<sub>A</sub>Rs are sufficiently sensitive to detect GABA spillover from neighboring inhibitory terminals (see also refs. 3,4), their affinity, estimated from pressure-applied GABA, was relatively low (half maximal effective concentration  $\approx$  60  $\mu$ M). Furthermore, the pharmacological profile was consistent with the

$\alpha_2$  subunit being present, which has been detected immunohistochemically at mossy fibers<sup>3</sup>, and is not thought to contribute to high-affinity receptors, implying that they may not be able to detect low ambient GABA concentrations.

Nevertheless, the identification of relatively low-affinity receptors (see also ref. 7) does not exclude the additional presence of high-affinity receptors. Dentate granule cells express tonically active  $\delta$  subunit-containing GABA<sub>A</sub>Rs in their somatodendritic compartment, which are sensitive to changes in ambient GABA<sup>8–10</sup>. Such receptors, which commonly contain  $\alpha_4$  subunits, are generally thought to be extrasynaptic, have a high affinity for GABA and exhibit relatively little desensitization<sup>9,11–13</sup>. They are also sensitive to the endogenous neurosteroid tetrahydrodeoxycorticosterone (THDOC) at nanomolar concentrations that occur in the brain<sup>14</sup> and to the hypnotic drug 4,5,6,7-tetrahydroisoxazolo[5,4-c]pyridin-3-ol (also known as gaboxadol, GBX). Although  $\alpha_4$  and  $\delta$  subunits are abundant in granule cell bodies and dendrites<sup>9,15</sup>, it is not known if either or both also occur in mossy fibers.

We found that GABA<sub>A</sub>Rs, tonically active in quiescent acute brain slices in the absence of added GABA, directly modulated mossy fiber membrane potentials, with a pharmacological profile that is consistent with  $\delta$  subunits being present, and affected spike properties and spike-driven Ca<sup>2+</sup> influx in individual boutons. We also found that potentiating and blocking high-affinity GABA<sub>A</sub>Rs had opposite effects on excitatory synaptic transmission to CA3 pyramidal cells. Finally, presynaptic GABA<sub>A</sub>Rs paradoxically facilitated the induction of long-term potentiation at mossy fiber synapses. Our results reveal an important mechanism by which information flow to the hippocampus can be bi-directionally modulated.

<sup>1</sup>Institute of Neurology, University College London, London, UK. <sup>2</sup>Department of Pharmacology, School of Pharmacy, University of London, London, UK. <sup>3</sup>Present address: Instituto de Neurociencias, CSIC & Universidad Miguel Hernández, Alicante, Spain. <sup>4</sup>These authors contributed equally to this work. Correspondence should be addressed to A.R. (arnaud.ruiz@pharmacy.ac.uk) or D.M.K. (d.kullmann@ion.ucl.ac.uk).

Received 25 September 2009; accepted 5 February 2010; published online 21 March 2010; doi:10.1038/nn.2512

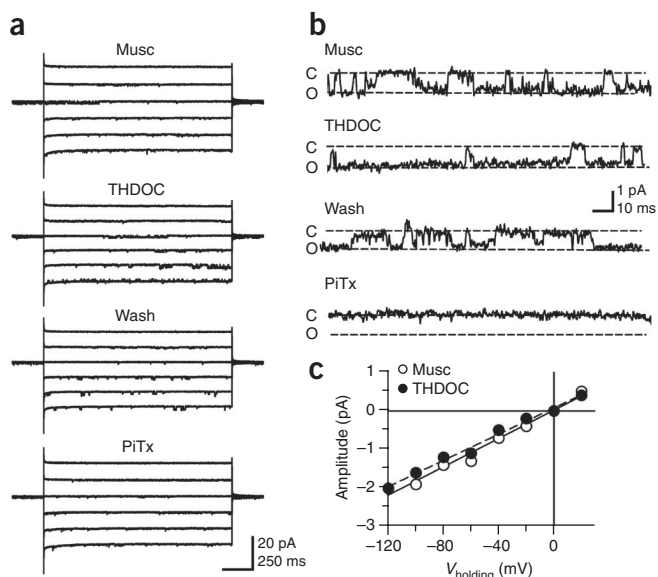


**Figure 1** THDOC modulates GABA<sub>A</sub> receptors in outside-out patches from mossy fiber boutons. (a) Traces obtained in one patch at different holding potentials (–120 to –20 mV) showing single-channel currents evoked by muscimol (10 μM, musc) and their reversible modulation by 10 nM THDOC (THDOC, wash) and block by 100 μM picrotoxin (PiTx). (b) High magnification of a portion of the traces shown in a demonstrating an increased open channel probability when THDOC was added to muscimol. C, closed; O, open. (c) The single-channel conductance calculated from the slope of the open channel current-voltage relationship was unaltered by THDOC (example from one patch).

## RESULTS

### High-affinity GABA<sub>A</sub>Rs affect mossy fiber excitability

We searched for δ subunit-containing GABA<sub>A</sub>Rs at mossy fibers by examining the effects of THDOC and of GBX on antidromic action current threshold in granule cells held in voltage clamp. Ionotropic glutamate and GABA<sub>B</sub> receptors were blocked throughout with 2,3-dihydroxy-6-nitro-7-sulfamoyl-benzo[f]quinoxaline (NBQX, 50 μM), D-2-amino-5-phosphonovalerate (AP5, 50 μM) and CGP52432 (5 μM). We measured the success rate for evoking action currents in response to electrical stimuli applied at different intensities via a bipolar electrode in stratum lucidum. Both THDOC (10 nM) and GBX (1 μM) reversibly decreased the action current success rate (**Supplementary Fig. 1**). For each condition, we estimated the stimulus intensity (in arbitrary units), yielding a 50% action current success rate (stim<sub>50</sub>). THDOC reversibly increased the action current threshold (stim<sub>50</sub> control, 3.7 ± 0.5; stim<sub>50</sub> THDOC, 7.4 ± 0.8; *n* = 8, mean ± s.e.m., paired *t* test, *P* < 0.01; **Supplementary Fig. 1**). Application of GBX had a similar effect (stim<sub>50</sub> control, 5.3 ± 0.3; stim<sub>50</sub> GBX, 7.5 ± 0.3; *n* = 4, *P* < 0.02). These results indicate that ligands selective for δ subunit-containing GABA<sub>A</sub>Rs reduce axonal excitability.

The whole-cell recording method can alter the intracellular chloride concentration ([Cl<sup>-</sup>]<sub>i</sub>) in the axon<sup>3</sup>. We therefore tested the effect of THDOC on action current success rate in granule cells using gramicidin perforated-patch recordings. THDOC had a similar effect on action current threshold in perforated-patch as with whole-cell recordings (stim<sub>50</sub> control, 1.6 ± 0.4; stim<sub>50</sub> THDOC, 3.6 ± 0.8; *n* = 3, *P* < 0.05, data not shown). Taken together with previous evidence that either activating or blocking GABA<sub>A</sub>Rs alters mossy fiber excitability in opposite directions depending on [Cl<sup>-</sup>]<sub>i</sub> (ref. 3), these results imply

that high-affinity neurosteroid-sensitive GABA<sub>A</sub>Rs have a profound effect on mossy fiber excitability in the absence of manipulations that increase ambient GABA.

### Presynaptic GABA<sub>A</sub>Rs at mossy fibers

Measurements of mossy fiber excitability do not give a quantitative indication of the effects of GABA<sub>A</sub>Rs on the presynaptic membrane potential. Furthermore, such experiments do not distinguish between receptors in presynaptic boutons and in the rest of the axon. We therefore obtained patch-clamp recordings from mossy fiber boutons<sup>16,17</sup> (**Supplementary Fig. 2**). Consistent with previous results<sup>6</sup>, the selective GABA<sub>A</sub> receptor agonist muscimol (10 μM) evoked channel currents in outside-out patches from mossy fiber boutons in the presence of a cocktail of blockers of ionotropic glutamate and GABA<sub>B</sub> receptors and voltage-dependent Ca<sup>2+</sup> (CdCl<sub>2</sub>, 100–200 μM) and Na<sup>+</sup> channels (TTX, 1 μM) (**Fig. 1a,b**). The modal single-channel conductance of GABA<sub>A</sub>Rs in mossy fiber boutons (γ<sub>MFB</sub>) estimated from the linear fit of the current-voltage relationship was 23.7 pS (*n* = 5; **Supplementary Fig. 3**), which was not significantly different from that measured in patches excised from granule cell bodies (γ<sub>GC</sub> = 27.1 pS, *n* = 7, *P* = 0.25). Application of picrotoxin (100 μM) blocked these currents, confirming that they were mediated by GABA<sub>A</sub>Rs (*n* = 3). THDOC (10 nM) increased the apparent open probability (baseline *P*<sub>open</sub>, 0.18 ± 0.02; THDOC *P*<sub>open</sub>, 0.33 ± 0.03; *n* = 4, *P* < 0.05), with no effect on the single-channel conductance (**Fig. 1c**).

Thus, at least some presynaptic GABA<sub>A</sub>Rs are modulated by neurosteroids. Because we selected patches in which single channel openings could be resolved and because the agonist was applied continuously, we could not determine the extent to which desensitizing THDOC-insensitive channels coexist.

### Presynaptic GABA<sub>A</sub>Rs depolarize boutons

Previous studies have suggested that GABA<sub>A</sub>Rs depolarize mossy fiber boutons<sup>4,6</sup>, consistent with the actions of presynaptic GABA<sub>A</sub>Rs elsewhere in the CNS<sup>1,2</sup>. However, the methods used have not allowed a direct estimate of the actions of GABA<sub>A</sub>Rs on the presynaptic membrane potential; whole-terminal recordings perturb both [K<sup>+</sup>]<sub>i</sub> and [Cl<sup>-</sup>]<sub>i</sub>, which interact to determine the driving force for GABA<sub>A</sub> receptor-mediated ion fluxes. We therefore applied ramp voltage commands in the cell-attached patch-clamp recording mode, with a pipette containing 155 mM [K<sup>+</sup>]<sub>i</sub>, which is close to [K<sup>+</sup>]<sub>i</sub> (refs. 18,19). Because the K<sup>+</sup> flux reverses when the pipette and intracellular potential are equal, this allows a minimally invasive estimate of the presynaptic membrane potential. Ramp voltage commands evoked an inward current that reversed polarity at -70.8 ± 3.3 mV (*n* = 19; **Fig. 2a**). We verified that this current was carried by K<sup>+</sup> ions; the inward component was attenuated when recording with a low [K<sup>+</sup>]<sub>i</sub> pipette solution (**Supplementary Fig. 4**). When the same method was used to estimate the membrane potential in dentate granule cell bodies, it yielded more negative values (-81.6 ± 2.6 mV, *n* = 21, *P* < 0.05; **Fig. 2b**).

We applied repeated ramp commands to investigate the effect of either activating or blocking GABA<sub>A</sub>Rs on the apparent membrane potential in mossy fiber boutons. Local pressure application of muscimol (10 μM, <150 μm from the bouton) depolarized boutons by 18.5 ± 3.7 mV (*n* = 4, *P* < 0.05; **Fig. 2c,d**). Conversely, pressure application of gabazine hyperpolarized boutons by 8.5 ± 4.5 mV (*n* = 6, *P* < 0.05; **Fig. 2c–f**). We verified that muscimol had no effect when GABA<sub>A</sub>Rs were pre-blocked with picrotoxin (-0.7 ± 1.4 mV, *n* = 3; **Fig. 2f**). Similarly, local pressure application of artificial CSF (ACSF) also had no substantial effect (3.3 mV ± 2.1 mV, *n* = 3; **Fig. 2f**), arguing against a movement artifact being the cause of the change in apparent bouton potential.

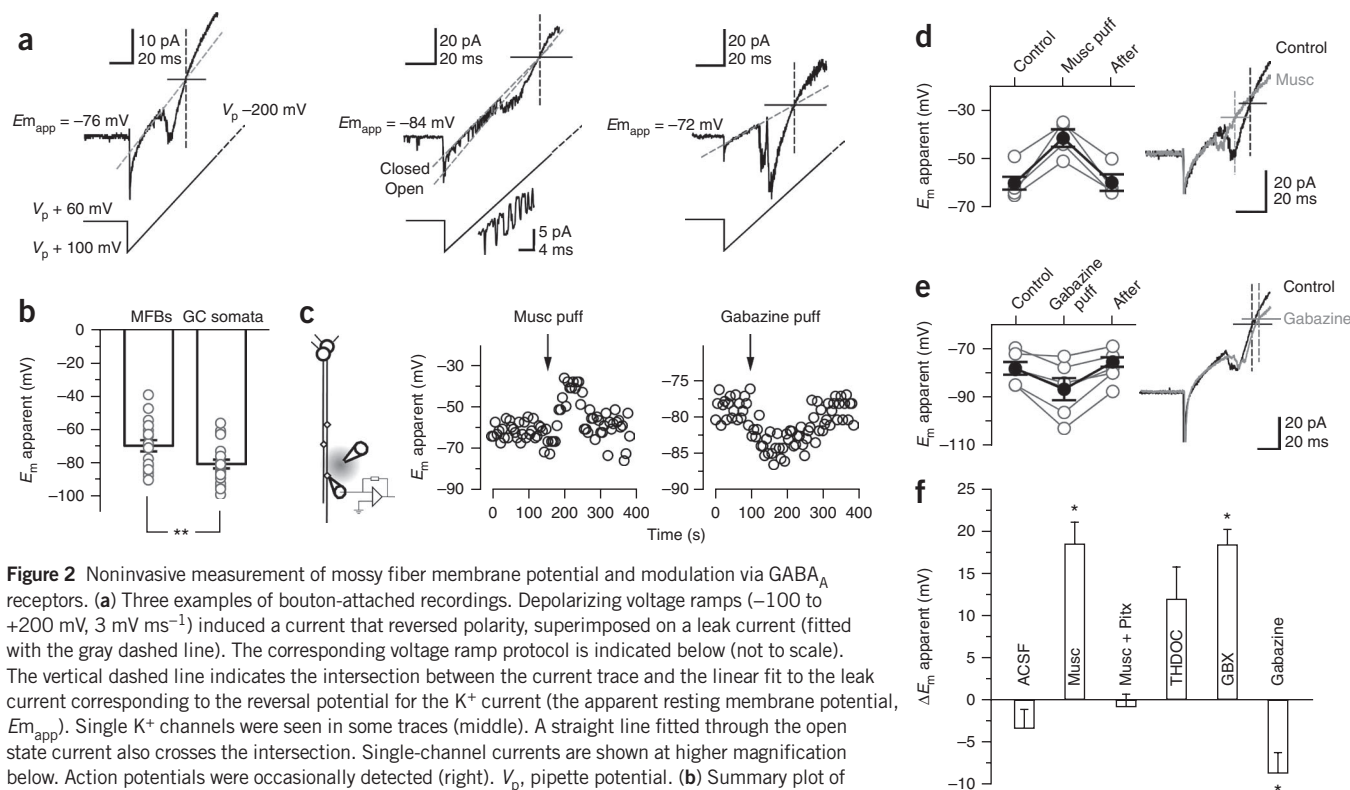


**Figure 2** Noninvasive measurement of mossy fiber membrane potential and modulation via GABA<sub>A</sub> receptors. **(a)** Three examples of bouton-attached recordings. Depolarizing voltage ramps ( $-100$  to  $+200$  mV,  $3$  mV  $ms^{-1}$ ) induced a current that reversed polarity, superimposed on a leak current (fitted with the gray dashed line). The corresponding voltage ramp protocol is indicated below (not to scale). The vertical dashed line indicates the intersection between the current trace and the linear fit to the leak current corresponding to the reversal potential for the K<sup>+</sup> current (the apparent resting membrane potential,  $E_{m,app}$ ). Single K<sup>+</sup> channels were seen in some traces (middle). A straight line fitted through the open state current also crosses the intersection. Single-channel currents are shown at higher magnification below. Action potentials were occasionally detected (right).  $V_p$ , pipette potential. **(b)** Summary plot of estimated membrane potential ( $E_m$  apparent) measured in bouton- and soma-attached recordings (error bars represent s.e.m.). The estimated membrane potential in mossy fiber boutons was more depolarized than that measured at granule cell somata (\*\* $P = 0.03$ , Mann-Whitney  $U$  test). **(c)** Left, experimental design used to measure the effect of muscimol or gabazine on bouton membrane potential. Right, apparent membrane potential in two mossy fiber boutons showing the effects of pressure application of muscimol (musc puff) or gabazine (gabazine puff), as indicated. **(d,e)** Effects of muscimol **(d)** and gabazine **(e)** on  $E_m$  apparent, with sample traces before (control, black) and immediately after (gray) drug application (averages of five consecutive trials). **(f)** Summary data for the effect of pressure application of ACSF ( $n = 3$ ), muscimol ( $n = 6$ ), muscimol in a background of picrotoxin ( $n = 6$ ), THDOC ( $n = 3$ ), GBX ( $n = 8$ ) and gabazine ( $n = 4$ ). (\* $P = 0.01$ , paired  $t$  test.)

Prompted by the evidence that  $\delta$ -containing receptors are present in boutons, we tested the effect of GBX. Local pressure application of GBX depolarized mossy fiber boutons by  $18.4 \pm 1.8$  mV ( $n = 8$ ,  $P < 0.05$ ; **Fig. 2f**). A similar trend was observed with THDOC application ( $12 \pm 4$  mV;  $n = 3$ ;  $P = 0.08$ ; **Fig. 2f**). Taken together, these results directly demonstrate that presynaptic GABA<sub>A</sub>Rs sensitive to  $\delta$ -selective agents have a depolarizing action when  $[K^+]_i$  and  $[Cl^-]_i$  are relatively unperturbed.

### Tonically active GABA<sub>A</sub>Rs alter spike shape

Although bouton-attached recordings provide a minimally invasive measurement of membrane potential, the high access resistance makes it difficult to record the action potential shape. We therefore used whole-bouton recordings to determine how tonic GABA<sub>A</sub> receptor-mediated depolarization might affect neurotransmitter release. Ionotropic glutamate and metabotropic GABA receptors were blocked with NBQX ( $50$   $\mu$ M), AP5 ( $50$   $\mu$ M) and CGP-52432 ( $5$   $\mu$ M). We initially voltage clamped boutons at  $-70$  mV with a cesium-based pipette solution containing  $155$  mM  $[Cl^-]$ . Application of picrotoxin ( $100$   $\mu$ M) or gabazine ( $5$  or  $10$   $\mu$ M) decreased the holding current at  $22$ – $24$   $^{\circ}C$  (picrotoxin,  $3.2 \pm 1.5$  pA,  $n = 7$ ; gabazine,  $5.1 \pm 1.7$  pA,  $n = 2$ ; **Fig. 3a,b**) and at  $32$   $^{\circ}C$  (gabazine,  $3.3 \pm 1.1$  pA,  $n = 3$ ; **Fig. 3c,d**). These results confirm that GABA<sub>A</sub>Rs in mossy fibers are tonically active in a quiescent slice. We then examined the role of the tonic GABA<sub>A</sub> conductance in action potentials by recording from mossy fiber boutons in current-clamp mode with a pipette containing  $155$  mM KCl at  $32$   $^{\circ}C$ . Blocking tonically active GABA<sub>A</sub>Rs with gabazine (**Fig. 4**) reversibly hyperpolarized all boutons recorded (control,  $-73.3 \pm 2.0$  mV; gabazine,  $-78.5 \pm 2.6$  mV;  $n = 8$ ,

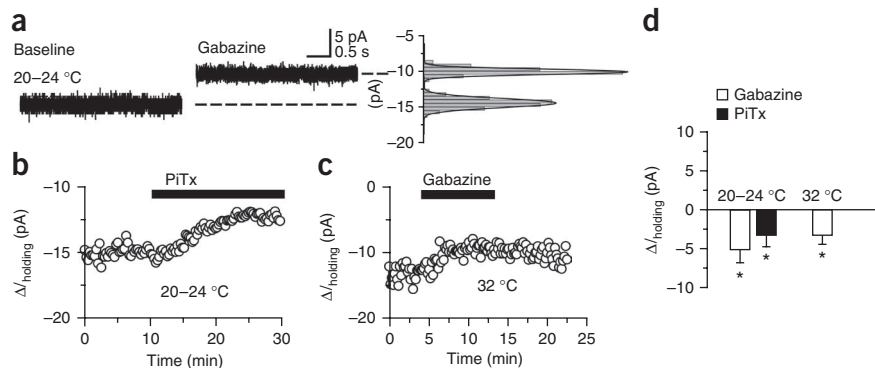


**Figure 3** Blocking GABA<sub>A</sub> receptors reveals a tonic current in mossy fiber boutons. **(a)** Whole-bouton voltage-clamp recording ( $-70$  mV) showing a  $4.5$  pA tonic current in the presence of gabazine ( $5$   $\mu$ M). Right, all-point histograms and Gaussian fits derived from the traces. **(b,c)** Time course of holding current in two mossy fiber boutons recorded at  $22$ – $24$   $^{\circ}C$  **(b)** and at  $32$   $^{\circ}C$  **(c)** showing the effect of blocking GABA<sub>A</sub> receptors with picrotoxin ( $100$   $\mu$ M) or gabazine ( $5$   $\mu$ M). **(d)** Summary of changes in holding current measured in mossy fiber boutons in experiments performed at  $22$ – $24$   $^{\circ}C$  and  $32$   $^{\circ}C$  ( $\pm$  s.e.m., \* $P < 0.05$ , paired  $t$  test).

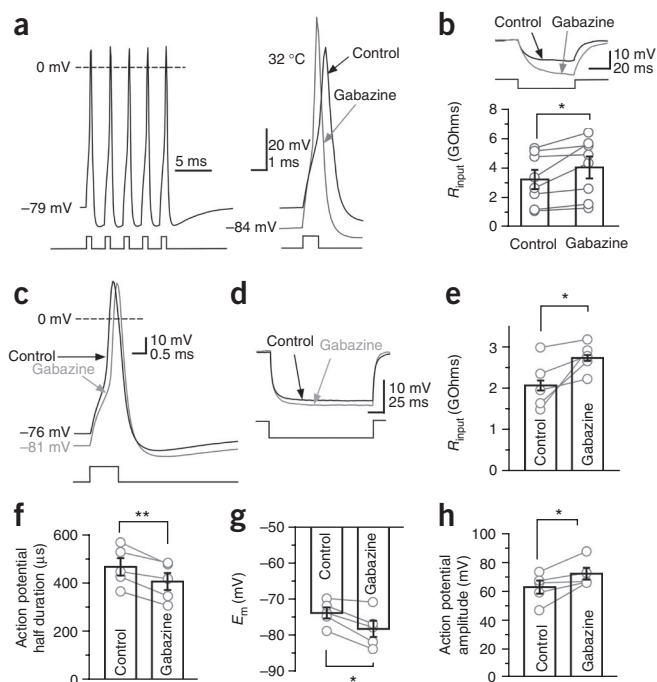


**Figure 4** Tonic GABA<sub>A</sub> receptor-mediated currents modulate the electrical properties of mossy fiber boutons. **(a)** Current-clamp recording from a mossy fiber bouton at 32 °C (155 mM KCl). Left, the bouton fired with high fidelity in response to five consecutive depolarizing pulses at 200 Hz (average of ten traces). Right, sample traces (averages of ten consecutive trials) showing the action potential before (black) and after (gray) superfusion of gabazine (5 μM). **(b)** Top, response to hyperpolarizing current injection showing an increase in input resistance in gabazine. Bottom, summary of changes in input resistance in mossy fiber boutons recorded with 155 mM [Cl<sup>-</sup>]<sub>i</sub>. **(c)** Current-clamp recording from a mossy fiber bouton with 20 mM [Cl<sup>-</sup>]<sub>i</sub>. Sample traces show the action potential (averages of ten consecutive trials) before (black) and after (gray) superfusion of gabazine (5 μM). **(d)** Response to hyperpolarizing current injection showing the increase in input resistance in gabazine (recording obtained with 20 mM [Cl<sup>-</sup>]<sub>i</sub>). **(e)** Summary plot of the effect of gabazine on input resistance. **(f-h)** Summary plots showing the effects of gabazine on action potential parameters measured in mossy fiber boutons with 20 mM [Cl<sup>-</sup>]<sub>i</sub>. Bars indicate mean ± s.e.m. and gray symbols indicate individual experiments (\**P* < 0.05, \*\**P* < 0.01, paired *t* test).

*P* < 0.004; **Fig. 4a** and **Supplementary Fig. 5**). This effect was accompanied by an increase in input resistance (control, 3.2 ± 0.6 GΩ; gabazine, 4.0 ± 0.7 GΩ; *P* < 0.03; **Fig. 4b**), an increase in the amplitude of the action potential (control, 85.9 ± 3.9 mV; gabazine, 95.1 ± 3.4 mV; *P* < 0.02) and an acceleration of its wave form (half-duration control, 504 ± 34 μs; gabazine, 423 ± 24 μs; *P* < 0.02) (**Fig. 4a** and **Supplementary Fig. 5**).

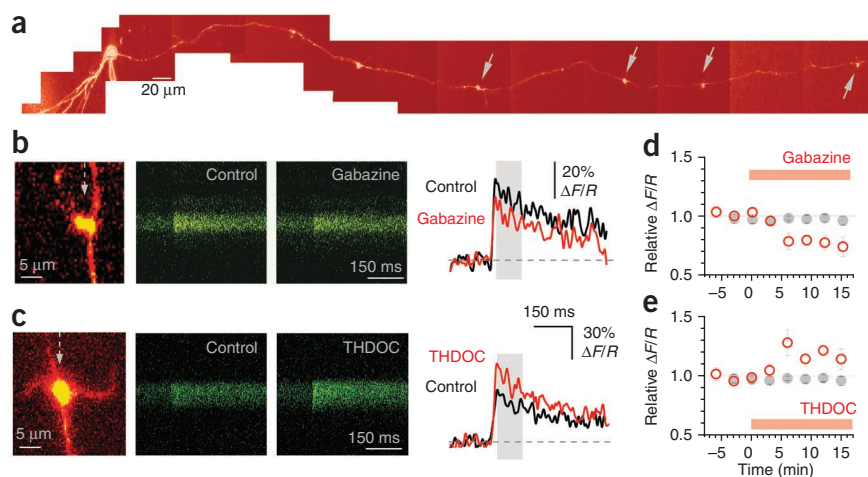
We again measured action potential waveforms with a lower internal chloride concentration (20 mM) to match estimates obtained at a brainstem synapse<sup>20</sup>. Gabazine applied at 32 °C hyperpolarized mossy fiber boutons (control, -74.0 ± 1.5 mV; gabazine, -78.4 ± 2.2 mV; *P* < 0.05; **Fig. 4c,g**) and increased their input resistance (control, 3.2 ± 0.6 MΩ; gabazine, 4.0 ± 0.7 MΩ; *P* < 0.05; **Fig. 4d,e**). This effect was accompanied by a reduction in the half duration of action potentials (control, 470 ± 36 μs; gabazine, 410 ± 35 μs; *P* < 0.01, *n* = 5;

**Fig. 4c,f**) and an increase in their amplitude (control, 62.3 ± 4.5 mV; gabazine, 71.5 ± 4.1 mV; *P* < 0.05; **Fig. 4h**). These effects were partly reversible on gabazine washout (membrane potential, -76 ± 2 mV; input resistance, 2.5 ± 0.4 MΩ; action potential half-duration, 430 ± 33 μs; action potential amplitude, 67.1 ± 3.7 mV). Thus, tonic activation of GABA<sub>A</sub>Rs can modulate both passive and active properties of mossy fiber boutons under relatively physiological conditions, with intact GABA uptake mechanisms.

### Tonically active GABA<sub>A</sub>Rs modulate Ca<sup>2+</sup> transients

How do tonically active GABA<sub>A</sub>Rs affect presynaptic Ca<sup>2+</sup> kinetics in mossy fiber boutons? We used two-photon excitation microscopy to identify individual giant boutons up to 1,000 μm from their parent granule cell body<sup>21–23</sup>. The whole-cell pipette contained both a fluorescent Ca<sup>2+</sup> indicator (Fluo-4) and a morphological tracer (Alexa Fluor 594). Giant mossy fiber boutons were unambiguously identified by their characteristic size and shape, including thin filopodial protrusions (**Fig. 5a–c**). Gabazine at near-physiological temperature (34 °C) had no consistent effect on the resting Ca<sup>2+</sup>-dependent fluorescence, but decreased the size of the action potential-dependent fluorescence transient ( $\Delta F/R$  = 83 ± 5% of baseline, *n* = 7, *P* = 0.032; **Fig. 5b,d**

**Figure 5** Tonically active neurosteroid-sensitive GABA<sub>A</sub> receptors enhance presynaptic action potential-dependent Ca<sup>2+</sup> transients in giant mossy fiber boutons. **(a)** Reconstruction of a dentate granule cell and its intact axon (Alexa Fluor 594 channel, λ<sub>exc</sub> = 800 nm). The somatic patch pipette is seen at left. The collage was obtained from Kalman-filtered averages of 10–15-μm stacks. Arrows indicate giant boutons equipped with characteristic thin filopodia. **(b)** Blocking GABA<sub>A</sub> receptors with gabazine reduced spike-dependent presynaptic Ca<sup>2+</sup> entry. Left, representative giant bouton (red Alexa channel, dotted arrow shows position of line scan). Line scans and traces are Ca<sup>2+</sup> responses in the mossy fiber bouton shown on the left (green Fluo-4 channel, 10-trace average, averaging window for  $\Delta F/R$  is indicated by the gray area) following a single action potential induced at the soma in control conditions and in 1-μM gabazine. **(c)** THDOC (10 nM) enhanced spike-dependent presynaptic Ca<sup>2+</sup> entry; data are presented as in **b**. **(d,e)** Summary of the effects of gabazine (*n* = 7, **d**) and THDOC (*n* = 8, **e**) on the average spike-evoked Ca<sup>2+</sup> response. Each point is the average of two trials. Gray symbols indicate the average  $\Delta F/R$  time course in control conditions (*n* = 7). Error bars represent s.e.m.



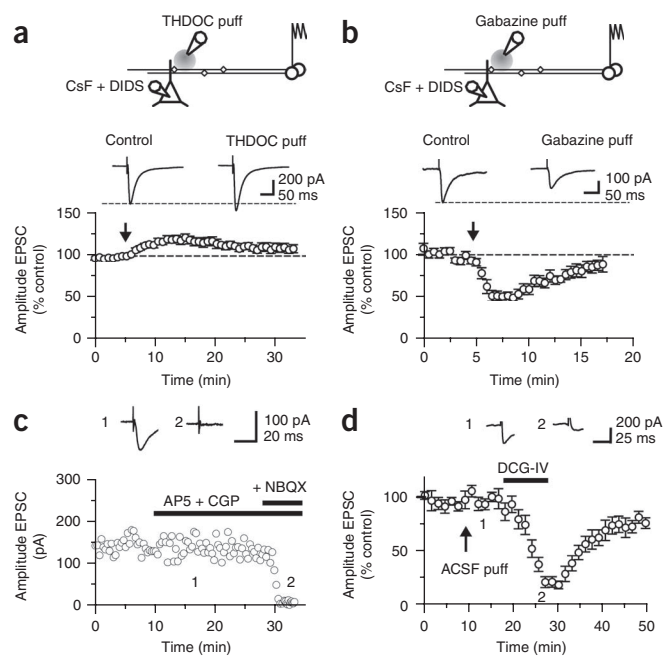


**Figure 6** Bidirectional modulation of synaptic transmission via tonically active GABA<sub>A</sub> receptors at mossy fibers. **(a)** Top, schematic illustrating the experimental design used to study presynaptic GABA<sub>A</sub> receptors at mossy fiber–CA3 synapses. Postsynaptic GABA<sub>A</sub> receptors in CA3 pyramidal cells were blocked using an intracellular pipette solution containing CsF and DIDS. A pressure-application pipette containing THDOC (50 nM, left) was positioned ~50–200 μm from the apical dendrite of the recorded neurons. Bottom, time course of the effects of pressure application of THDOC ( $n = 8$ ). Traces are averages of ten consecutive EPSCs before and after drug application. NMDA and GABA<sub>B</sub> receptors were blocked throughout. **(b)** Effect of gabazine (10 μM) applied as in **a** ( $n = 6$ ). **(c)** Plot of evoked postsynaptic current amplitude against time in control experiments showing the complete blockade of synaptic transmission on NBQX (20 μM) application. Sample traces (averages of ten consecutive EPSCs) were taken as indicated on the graph. **(d)** Time course of the effects of pressure application of ACSF (arrow) followed by superfusion of DCG-IV (1 μM) on evoked EPSCs recorded with a pipette solution containing CsF and DIDS ( $n = 5$ ). Sample traces show the average of ten consecutive EPSCs before and after superfusion of DCG-IV. Error bars represent s.e.m.

1 μM) depressed evoked EPSCs by  $82 \pm 4\%$  ( $n = 4$ ; **Fig. 6d**), indicating that they originated from mossy fibers. Finally, neither THDOC nor gabazine affected the input resistance of CA3 pyramidal neurons.

Neurosteroid-sensitive GABA<sub>A</sub>Rs thus exert a bidirectional modulatory influence on mossy fiber transmission to CA3 pyramidal neurons. We asked whether tonically active GABA<sub>A</sub>Rs have a different effect on mossy fiber transmission to interneurons in stratum lucidum (with DCG-IV applied at the end of the experiment to verify that EPSCs were sensitive). Although gabazine had a qualitatively similar effect, the depression of mossy fiber EPSCs in interneurons was smaller on average than in CA3 pyramidal neurons ( $25 \pm 9\%$ ,  $n = 9$ ,  $P < 0.05$ , data not shown) and was also more variable, ranging from 0 to 81%. We did not attempt to identify interneurons to determine whether this variability correlated with morphological or other parameters. Finally, in a separate set of experiments, we recorded EPSCs in CA3 pyramidal neurons under identical conditions, but which were evoked via an electrode positioned in stratum radiatum to elicit action potentials in associational–commissural axons, which include recurrent collaterals of CA3 pyramidal cells. In contrast with the robust effect on mossy fiber–evoked EPSCs, gabazine did not affect the EPSC amplitude ( $95 \pm 14\%$  of baseline,  $P = 0.73$ ,  $n = 4$ ; **Supplementary Fig. 7**).

### Presynaptic GABA<sub>A</sub>Rs facilitate LTP induction

Mossy fibers exhibit NMDA receptor–independent LTP, the induction of which is sensitive to the presynaptic membrane potential<sup>26</sup>. The depolarizing action of GABA<sub>A</sub>Rs in mossy fibers suggests that they may facilitate LTP induction by enhancing presynaptic Ca<sup>2+</sup> influx. Although presynaptic Ca<sup>2+</sup> transients in individual boutons evoked by single action potentials were attenuated by blocking GABA<sub>A</sub>Rs (**Fig. 5d**), this finding cannot necessarily be extrapolated to high-frequency trains of action potentials in multiple axons, which are required to induce LTP at mossy fibers. We therefore asked whether local pressure application of gabazine immediately before high-frequency stimulation (HFS, 100 Hz, 200 ms) in the dentate gyrus could interfere with Ca<sup>2+</sup>-dependent fluorescence signals detected with the high-affinity ratiometric indicator Fura-2 bulk-loaded to multiple axons in stratum lucidum. The indicator was delivered by injection of the acetoxymethyl (AM) ester close to the site of stimulation<sup>27</sup>. We then waited for it to be taken up by mossy fibers and to diffuse to stratum lucidum in CA3 before delivering HFS trains at 32 °C, with glutamate receptors being blocked by NBQX and AP5. Because HFS-evoked Ca<sup>2+</sup> signals (estimated from the fluorescence

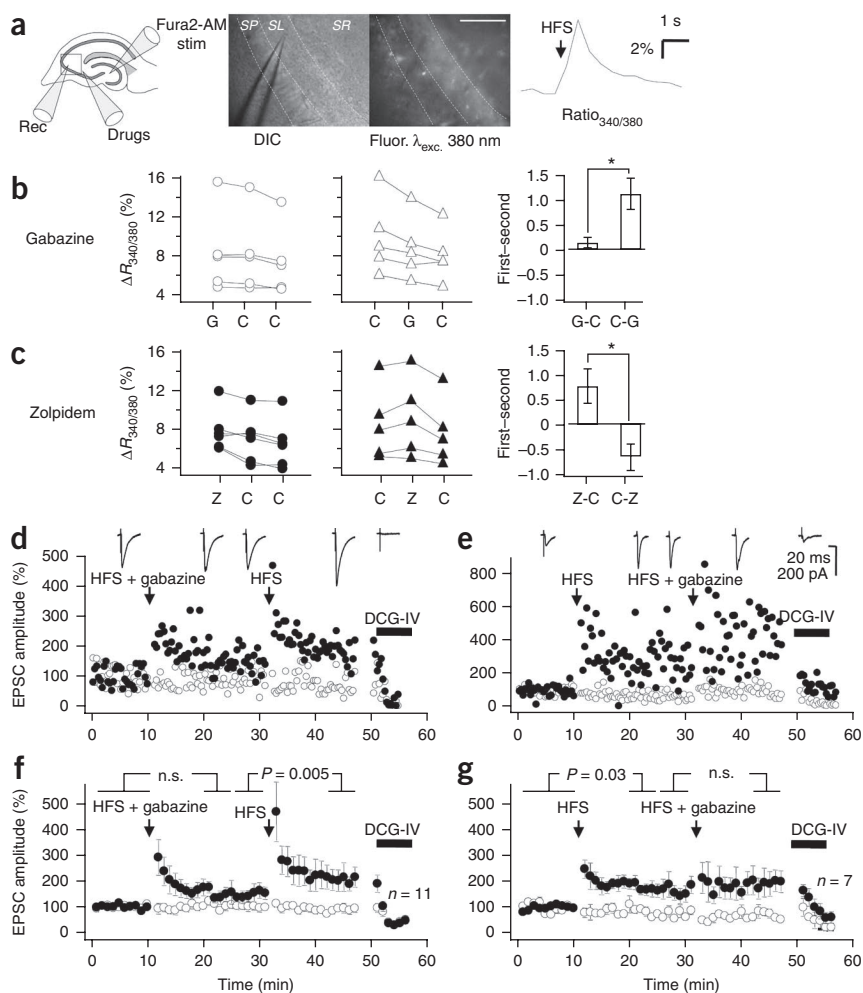
and Online Methods). In contrast, THDOC (10 nM) increased the action potential–dependent fluorescence signal ( $\Delta F/R = 114 \pm 5\%$  of baseline,  $n = 8$ ,  $P = 0.021$ ), with no consistent effect on the resting fluorescence (**Fig. 5c,e**).

These results imply that tonically active GABA<sub>A</sub>Rs normally enhance the Ca<sup>2+</sup> influx that accompanies action potentials and that this phenomenon can be potentiated by endogenous neurosteroids acting on  $\delta$  subunit–containing GABA<sub>A</sub>Rs. Taken together with the results of direct mossy fiber bouton recordings (**Fig. 4**), these effects are consistent with the observation that Ca<sup>2+</sup> influx is positively correlated with action potential width<sup>17,24</sup>. In contrast with mossy fiber boutons, action potential–dependent fluorescence transients in boutons of CA3 pyramidal cell axons, recorded under identical conditions, were unaffected by gabazine ( $n = 8$ ) or THDOC ( $n = 6$ ; see **Supplementary Fig. 6**), implying that tonically active GABA<sub>A</sub>Rs are not ubiquitously expressed in hippocampal glutamatergic boutons.

### Presynaptic GABA<sub>A</sub>Rs enhance synaptic transmission

How do tonically active GABA<sub>A</sub>Rs affect excitatory synaptic transmission to CA3 pyramidal neurons? We recorded from pyramidal neurons with a pipette solution containing CsF and 4,4′-diisothiocyanostilbene-2,2′-disulfonic acid (DIDS) to block postsynaptic GABA<sub>A</sub>Rs intracellularly<sup>25</sup> while leaving presynaptic receptors intact. Mossy fibers were stimulated in stratum granulosum and a pressure-application pipette containing THDOC or gabazine was positioned in stratum lucidum near the apical dendrite of the recorded CA3 pyramidal neuron. We thus avoided potential effects of manipulating GABA<sub>A</sub>Rs at the site of axon recruitment by the electrical stimulus. Local pressure application of THDOC (50 nM, 10–30 psi, 150–300 ms) reversibly increased the EPSC amplitude by  $22 \pm 4\%$  ( $n = 8$ ;  $P < 0.03$ ; **Fig. 6a**). Conversely, pressure ejection of gabazine reversibly decreased the EPSC amplitude by  $44 \pm 6\%$  ( $n = 6$ ,  $P < 0.01$ ; **Fig. 6b**). Superfusion of NBQX (20 μM) completely abolished residual EPSCs, confirming that they were mediated by AMPA/kainate receptors ( $n = 3$ ; **Fig. 6c**). We did not detect any effect of puffing ACSF ( $n = 5$ ; **Fig. 6d**), arguing against movement artifacts being involved. Superfusion of the group II–selective metabotropic glutamate receptor agonist DCG-IV ((2S,2′R,3′R)-2-(2′,3′-dicarboxycyclopropyl)glycine,

**Figure 7** GABA<sub>A</sub> receptors facilitate mossy fiber LTP. **(a)** Schematic (left) and infrared differential interference contrast and fluorescence images (middle), illustrating the Fura2 imaging. A recording electrode (rec) was used to monitor mossy fiber excitatory postsynaptic potentials before glutamate receptor blockade and imaging. Mossy fibers were loaded (Fura2-AM) and stimulated (stim) in the dentate gyrus. Gabazine, zolpidem or vehicle were pressure applied just outside the imaged field (drugs). Scale bar represents 100  $\mu$ m. Right, sample Ca<sup>2+</sup> fluorescence trace showing a transient increase in the fluorescence ratio excited at 340 and 380 nm evoked by HFS. **(b)** Gabazine was pressure applied immediately before the first (left) or second (middle) of three trains delivered with 4-min intervals. The HFS-evoked fluorescence ratio transient ( $\Delta R_{340/380}$ ) was significantly attenuated ( $P < 0.02$ ) by gabazine (G), as revealed by comparing with control conditions (C, right). \* $P < 0.05$ . **(c)** Pressure-applied zolpidem (Z) increased the HFS-evoked fluorescence ratio transient ( $\Delta R_{340/380}$ ). \* $P < 0.05$ . **(d)** EPSC amplitudes recorded in a CA3 pyramidal neuron in response to stimulation of two pathways. HFS was delivered to one pathway (filled symbols) at the times indicated, either together with local pressure application of gabazine in stratum lucidum (HFS + gabazine) or alone (HFS). DCG-IV was applied at the end of the experiment to confirm that the responses were profoundly depressed, typical of mossy fibers. The sample traces were obtained in the test pathway, aligned with the times at which they were recorded. **(e)** Example of a cell in which the LTP induction protocols were applied in reverse order. **(f)** Average time course of 11 experiments; data are presented as in **d**. **(g)** Average time course of seven experiments; data are presented as in **e**. Error bars indicate s.e.m.



ratio excited at 340 nm and 380 nm) decreased in peak amplitude with repeated trials (as a result of photobleaching and continued redistribution of Fura-2), we alternately applied gabazine by local pressure either on the first trial or on the second trial in interleaved paired-trial experiments (Fig. 7a). The HFS-evoked Ca<sup>2+</sup> signal decreased significantly more when gabazine was applied on the second trial ( $\Delta R_{340/380}$ , first trial – second trial =  $1.13 \pm 0.31\%$ ,  $n = 5$ ) than when it was applied on the first trial ( $0.16 \pm 0.12\%$ ,  $n = 5$ ,  $P < 0.02$ ; Fig. 7b) in the pair. Although this result is consistent with a facilitatory role of GABA<sub>A</sub>Rs in presynaptic Ca<sup>2+</sup> signaling, it does not necessarily indicate that high-affinity receptors mediate the effect, as GABA released by the stimulus could have activated low-affinity receptors<sup>4,28</sup>. Indeed, when the benzodiazepine agonist zolpidem was applied immediately before the HFS, it had the opposite effect to gabazine (zolpidem on first trial,  $\Delta R_{340/380}$ , first trial – second trial =  $0.77 \pm 0.17\%$ ,  $n = 6$ ; zolpidem on second trial,  $-0.66 \pm 0.26\%$ ,  $n = 5$ ,  $P = 0.011$ ; Fig. 7c).

Notwithstanding the confounding effect of different subtypes of GABA<sub>A</sub>Rs present in mossy fibers (see also refs. 6,7), the small, but significant, effect of gabazine on HFS-evoked Ca<sup>2+</sup> signaling suggests that they may modulate the induction of LTP. To test this hypothesis, we attempted to elicit LTP at mossy fiber synapses by recording EPSCs in CA3 pyramidal neurons at 32 °C (Fig. 7d–g). A second pathway acted as a control for nonspecific changes in recording condition. AP5 was included in the perfusion solution and 5 mM EGTA in the pipette solution. We delivered HFS (100 Hz, 1 s) to the mossy fiber pathway, immediately following local pressure application of gabazine

in stratum lucidum in the vicinity of the recorded CA3 pyramidal neuron. This yielded a nonsignificant increase in EPSC amplitude ( $P = 0.12$ ,  $n = 11$ ; Fig. 7d,f). When the HFS was subsequently delivered to the same pathway without gabazine, robust LTP was elicited ( $P = 0.005$ ), reaching  $205 \pm 39\%$  of the baseline amplitude.

In a separate set of experiments, we inverted the order of conditioning stimuli, initially delivering HFS without gabazine and then repeating it, after an identical delay, with pressure-applied gabazine. In this case, LTP was readily elicited by HFS alone ( $170 \pm 25\%$ ,  $n = 6$ ,  $P = 0.03$ ). HFS repeated with gabazine elicited a small additional potentiation that did not reach significance ( $P > 0.05$ ; Fig. 7e,g). Although this experiment did not distinguish between tonically active receptors and lower-affinity receptors activated on tetanization, the effect of gabazine argues that mossy fiber LTP is indeed facilitated by GABA<sub>A</sub>Rs. Because postsynaptic depolarization has little or no role in mossy fiber LTP induction<sup>29</sup>, these results suggest that presynaptic GABA<sub>A</sub>Rs are involved in glutamatergic synaptic plasticity.

## DISCUSSION

We found that tonically active and neurosteroid-sensitive GABA<sub>A</sub> receptors enhanced neurotransmitter release in the brain by affecting action potential shape and Ca<sup>2+</sup> signaling. We also found that GABA<sub>A</sub>Rs facilitated the induction of a presynaptic form of LTP. It is highly unlikely that our findings of tonically active presynaptic GABA<sub>A</sub>Rs can be explained by a remote effect of GABA<sub>A</sub>Rs in the somato-dendritic compartments or axon initial segment. First, although subthreshold depolarization

can propagate a long distance in mossy fibers<sup>22,30</sup>, only a minority of axons supplying giant boutons are preserved during slice preparation. Mossy fibers were connected to their parent granule cells in experiments on action current threshold and Ca<sup>2+</sup> imaging in individual boutons, but these were carried out under somatic voltage clamp. Second, the bidirectional modulation of mossy fiber membrane potential and synaptic transmission to CA3 was achieved by locally applied gabazine or THDOC. Finally, we found THDOC-sensitive channels in outside-out patches excised from giant boutons. These results indicate that tonically active neurosteroid-sensitive receptors are present in the synaptic varicosities that synapse on CA3 pyramidal neurons. Although previous studies<sup>6</sup> have reported zolpidem-sensitive receptors with intermediate GABA sensitivity, as expected for  $\alpha_2$  and  $\gamma$ -subunit-containing receptors (see also ref. 3), these studies found no effect of blocking GABA<sub>A</sub>Rs on the input resistance of mossy fiber boutons unless GABA uptake was inhibited. A possible explanation for this discrepancy is that the input resistance is relatively insensitive to GABA<sub>A</sub> receptor manipulation, as compared with the holding current and membrane potential. In any case, the presence of zolpidem-sensitive receptors does not exclude the additional presence of high-affinity receptors. A further possibility is that the same receptors might be sensitive to both zolpidem and THDOC. Although such GABA<sub>A</sub>Rs have not been reported, stoichiometries with unusual pharmacological profiles have been identified in extrasynaptic membranes of hippocampal neurons<sup>31,32</sup> and diazepam has been reported to modulate GABA<sub>A</sub> receptor openings in the absence of GABA (ref. 33).

Our bouton-attached recordings minimized perturbation of [K<sup>+</sup>]<sub>i</sub> and [Cl<sup>-</sup>]<sub>i</sub>. The resting apparent membrane potential in boutons was estimated around -70 mV, about 10 mV above that of granule cell somata. Although a leak conductance through the patch can bias the estimate of the membrane potential<sup>34</sup>, this potential artifact had little effect on the qualitative effects of either blocking tonically active GABA<sub>A</sub>Rs with gabazine or potentiating them with THDOC. These manipulations altered the mossy fiber bouton membrane potential in opposite directions, indicating that the GABA<sub>A</sub> reversal potential was depolarized relative to the resting membrane potential. This finding is consistent with depolarizing actions of presynaptic GABA<sub>A</sub>Rs elsewhere in the CNS and implies that Cl<sup>-</sup> extrusion mechanisms are unable to drive the reversal potential for Cl<sup>-</sup> down to that for K<sup>+</sup> (ref. 20).

In the spinal cord, presynaptic GABA<sub>A</sub> receptor-mediated depolarization of primary afferents is accompanied by a depression of neurotransmitter release, secondary to Na<sup>+</sup> and/or Ca<sup>2+</sup> channel inactivation and action potential propagation failure<sup>1</sup>. In contrast, presynaptic depolarization at most sites studied in the brain, caused by GABA<sub>A</sub>, glycine or kainate receptor activation<sup>35–38</sup> or as a result of electrotonic propagation of subthreshold somatic depolarization<sup>22,30,39</sup>, is accompanied by enhanced evoked neurotransmitter release (although see ref. 40). Blocking tonically active GABA<sub>A</sub>Rs decreased spike half-width and action potential-dependent presynaptic Ca<sup>2+</sup> transients that were monitored with multi-photon excitation fluorescence microscopy. The change in action potential shape is consistent with de-inactivation of K<sup>+</sup> channels secondary to hyperpolarization. Because a linear dependence of Ca<sup>2+</sup> influx on action potential half-width has been reported in mossy fiber boutons<sup>17,24</sup>, this provides a ready explanation for the observed effects on glutamate release and orthodromic transmission to CA3 pyramidal neurons. However, the relationship between presynaptic membrane potential and exocytosis is affected by several other processes<sup>22,41–43</sup>, the relative contributions of which were beyond the scope of this study.

The effects of gabazine on mossy fiber bouton membrane potential, action potential shape and orthodromic transmission imply that the low ambient GABA level in a quiescent slice is sufficient for baseline activity of high-affinity receptors. The extracellular GABA concentration in the intact brain is difficult to measure, but estimates as high as 2–4  $\mu$ M have been obtained with microdialysis<sup>44</sup>. It may also fluctuate with behavioral state<sup>45</sup>. Taken together with evidence that neurosteroid levels fluctuate extensively in normal and pathological situations<sup>14,46</sup>, our results reveal a powerful mechanism for bidirectional modulation of mossy fiber transmission to CA3. Notably, although tonically active GABA<sub>A</sub>Rs in the somatodendritic compartment reduce granule cell excitability<sup>47,48</sup>, they enhance glutamate release from mossy fiber terminals, arguing against ‘tonic inhibition’ being synonymous with the action of these receptors.

We found that blocking GABA<sub>A</sub>Rs impaired the induction of mossy fiber LTP. Although we cannot rule out a more complex cascade, whereby GABA<sub>A</sub>Rs affect the release of a neuromodulator, which in turn alters the induction of LTP, our results are most simply interpreted as an effect on presynaptic receptors on mossy fibers themselves. Indeed, our results are consistent with the finding that manipulations that depolarize presynaptic boutons facilitate mossy fiber LTP induction<sup>26</sup>. The dual role of presynaptic GABA<sub>A</sub>Rs in modulating transmission and LTP at this synapse parallels the effects reported for presynaptic kainate receptors. Although we did not determine whether this effect is mediated by tonically active receptors or by lower affinity receptors recruited by tetanic stimulation, it further underlines the notion that presynaptic GABA<sub>A</sub> receptors have a paradoxical pro-excitatory role.

## METHODS

Methods and any associated references are available in the online version of the paper at <http://www.nature.com/natureneuroscience/>.

*Note: Supplementary information is available on the Nature Neuroscience website.*

## ACKNOWLEDGMENTS

We are grateful to P. Jonas and to D. Engel for help in optimizing mossy fiber bouton recordings and to C. Henneberger, M.C. Walker and K. Volynski for comments on the manuscript. This work was supported by the Medical Research Council (UK), the Wellcome Trust, the European Research Council and the Fondation pour la Recherche Médicale (France).

## AUTHOR CONTRIBUTIONS

A.R., E.C. and R.S.S. conducted the experiments. A.R. and E.C. analyzed the electrophysiology and epifluorescence imaging data. R.S.S. and D.A.R. analyzed the multi-photon imaging data. A.R., R.S.S., D.A.R. and D.M.K. conceived the study. D.M.K. wrote the first draft of the manuscript, which was revised by all of the authors.

## COMPETING FINANCIAL INTERESTS

The authors declare no competing financial interests.

Published online at <http://www.nature.com/natureneuroscience/>.

Reprints and permissions information is available online at <http://www.nature.com/reprintsandpermissions/>.

1. Kullmann, D.M. *et al.* Presynaptic, extrasynaptic and axonal GABA<sub>A</sub> receptors in the CNS: where and why? *Prog. Biophys. Mol. Biol.* **87**, 33–46 (2005).
2. Trigo, F.F., Marty, A. & Stell, B.M. Axonal GABA<sub>A</sub> receptors. *Eur. J. Neurosci.* **28**, 841–848 (2008).
3. Ruiz, A. *et al.* GABA<sub>A</sub> receptors at hippocampal mossy fibers. *Neuron* **39**, 961–973 (2003).
4. Nakamura, M., Sekino, Y. & Manabe, T. GABAergic interneurons facilitate mossy fiber excitability in the developing hippocampus. *J. Neurosci.* **27**, 1365–1373 (2007).
5. Jang, I.S., Nakamura, M., Ito, Y. & Akaike, N. Presynaptic GABA<sub>A</sub> receptors facilitate spontaneous glutamate release from presynaptic terminals on mechanically dissociated rat CA3 pyramidal neurons. *Neuroscience* **138**, 25–35 (2006).
6. Alle, H. & Geiger, J.R.P. GABAergic spill-over transmission onto hippocampal mossy fiber boutons. *J. Neurosci.* **27**, 942–950 (2007).

7. Han, J.W. *et al.* Differential pharmacological properties of GABA(A) receptors in axon terminals and soma of dentate gyrus granule cells. *J. Neurochem.* **109**, 995–1007 (2009).
8. Chandra, D. *et al.* GABA<sub>A</sub> receptor alpha 4 subunits mediate extrasynaptic inhibition in thalamus and dentate gyrus and the action of gaboxadol. *Proc. Natl. Acad. Sci. USA* **103**, 15230–15235 (2006).
9. Wei, W., Zhang, N., Peng, Z., Houser, C.R. & Mody, I. Perisynaptic localization of delta subunit-containing GABA(A) receptors and their activation by GABA spillover in the mouse dentate gyrus. *J. Neurosci.* **23**, 10650–10661 (2003).
10. Stell, B.M., Brickley, S.G., Tang, C.Y., Farrant, M. & Mody, I. Neuroactive steroids reduce neuronal excitability by selectively enhancing tonic inhibition mediated by delta subunit-containing GABA<sub>A</sub> receptors. *Proc. Natl. Acad. Sci. USA* **100**, 14439–14444 (2003).
11. Mangan, P.S. *et al.* Cultured hippocampal pyramidal neurons express two kinds of GABA<sub>A</sub> receptors. *Mol. Pharmacol.* **67**, 775–788 (2005).
12. Nusser, Z., Sieghart, W. & Somogyi, P. Segregation of different GABA<sub>A</sub> receptors to synaptic and extrasynaptic membranes of cerebellar granule cells. *J. Neurosci.* **18**, 1693–1703 (1998).
13. Wohlfarth, K.M., Bianchi, M.T. & Macdonald, R.L. Enhanced neurosteroid potentiation of ternary GABA(A) receptors containing the delta subunit. *J. Neurosci.* **22**, 1541–1549 (2002).
14. Belelli, D. & Lambert, J.J. Neurosteroids: endogenous regulators of the GABA(A) receptor. *Nat. Rev. Neurosci.* **6**, 565–575 (2005).
15. Sperk, G., Schwarzer, C., Tsunashima, K., Fuchs, K. & Sieghart, W. GABA(A) receptor subunits in the rat hippocampus I: immunocytochemical distribution of 13 subunits. *Neuroscience* **80**, 987–1000 (1997).
16. Bischofberger, J., Engel, D., Li, L., Geiger, J.R.P. & Jonas, P. Patch-clamp recording from mossy fiber terminals in hippocampal slices. *Nat. Protoc.* **1**, 2075–2081 (2006).
17. Geiger, J.R. & Jonas, P. Dynamic control of presynaptic Ca(2+) inflow by fast-inactivating K(+) channels in hippocampal mossy fiber boutons. *Neuron* **28**, 927–939 (2000).
18. Fricker, D., Verheugen, J.A. & Miles, R. Cell-attached measurements of the firing threshold of rat hippocampal neurons. *J. Physiol. (Lond.)* **517**, 791–804 (1999).
19. Verheugen, J.A., Fricker, D. & Miles, R. Noninvasive measurements of the membrane potential and GABAergic action in hippocampal interneurons. *J. Neurosci.* **19**, 2546–2555 (1999).
20. Price, G.D. & Trussell, L.O. Estimate of the chloride concentration in a central glutamatergic terminal: a gramicidin perforated-patch study on the calyx of Held. *J. Neurosci.* **26**, 11432–11436 (2006).
21. Scott, R. & Rusakov, D.A. Main determinants of presynaptic Ca<sup>2+</sup> dynamics at individual mossy fiber–CA3 pyramidal cell synapses. *J. Neurosci.* **26**, 7071–7081 (2006).
22. Scott, R., Ruiz, A., Henneberger, C., Kullmann, D.M. & Rusakov, D.A. Analog modulation of mossy fiber transmission is uncoupled from changes in presynaptic Ca<sup>2+</sup>. *J. Neurosci.* **28**, 7765–7773 (2008).
23. Scott, R., Lalic, T., Kullmann, D.M., Capogna, M. & Rusakov, D.A. Target-cell specificity of kainate autoreceptor and Ca<sup>2+</sup> store-dependent short-term plasticity at hippocampal mossy fiber synapses. *J. Neurosci.* **28**, 13139–13149 (2008).
24. Bischofberger, J., Geiger, J.R.P. & Jonas, P. Timing and efficacy of Ca<sup>2+</sup> channel activation in hippocampal mossy fiber boutons. *J. Neurosci.* **22**, 10593–10602 (2002).
25. Yakushiji, T., Tokutomi, N., Akaike, N. & Carpenter, D.O. Antagonists of GABA responses, studied using internally perfused frog dorsal root ganglion neurons. *Neuroscience* **22**, 1123–1133 (1987).
26. Schmitz, D., Mellor, J., Breusted, J. & Nicoll, R.A. Presynaptic kainate receptors impart an associative property to hippocampal mossy fiber long-term potentiation. *Nat. Neurosci.* **6**, 1058–1063 (2003).
27. Regehr, W.G. & Tank, D.W. The maintenance of LTP at hippocampal mossy fiber synapses is independent of sustained presynaptic calcium. *Neuron* **7**, 451–459 (1991).
28. Walker, M.C., Ruiz, A. & Kullmann, D.M. Monosynaptic GABAergic signaling from dentate to CA3 with a pharmacological and physiological profile typical of mossy fiber synapses. *Neuron* **29**, 703–715 (2001).
29. Nicoll, R.A. & Schmitz, D. Synaptic plasticity at hippocampal mossy fiber synapses. *Nat. Rev. Neurosci.* **6**, 863–876 (2005).
30. Alle, H. & Geiger, J.R.P. Combined analog and action potential coding in hippocampal mossy fibers. *Science* **311**, 1290–1293 (2006).
31. Glykys, J. & Mody, I. Activation of GABA<sub>A</sub> receptors: views from outside the synaptic cleft. *Neuron* **56**, 763–770 (2007).
32. Mortensen, M. & Smart, T.G. Extrasynaptic alphabeta subunit GABA<sub>A</sub> receptors on rat hippocampal pyramidal neurons. *J. Physiol. (Lond.)* **577**, 841–856 (2006).
33. Birnir, B., Eghbali, M., Everitt, A.B. & Gage, P.W. Bicuculline, pentobarbital and diazepam modulate spontaneous GABA(A) channels in rat hippocampal neurons. *Br. J. Pharmacol.* **131**, 695–704 (2000).
34. Chavas, J. & Marty, A. Coexistence of excitatory and inhibitory GABA synapses in the cerebellar interneuron network. *J. Neurosci.* **23**, 2019–2031 (2003).
35. Schmitz, D., Mellor, J. & Nicoll, R.A. Presynaptic kainate receptor mediation of frequency facilitation at hippocampal mossy fiber synapses. *Science* **291**, 1972–1976 (2001).
36. Stell, B.M., Rostaing, P., Triller, A. & Marty, A. Activation of presynaptic GABA(A) receptors induces glutamate release from parallel fiber synapses. *J. Neurosci.* **27**, 9022–9031 (2007).
37. Trigo, F.F., Chat, M. & Marty, A. Enhancement of GABA release through endogenous activation of axonal GABA(A) receptors in juvenile cerebellum. *J. Neurosci.* **27**, 12452–12463 (2007).
38. Turecek, R. & Trussell, L.O. Presynaptic glycine receptors enhance transmitter release at a mammalian central synapse. *Nature* **411**, 587–590 (2001).
39. Shu, Y., Hasenstaub, A., Duque, A., Yu, Y. & McCormick, D.A. Modulation of intracortical synaptic potentials by presynaptic somatic membrane potential. *Nature* **441**, 761–765 (2006).
40. Zhang, S.J. & Jackson, M.B. GABA-activated chloride channels in secretory nerve endings. *Science* **259**, 531–534 (1993).
41. Huang, H. & Trussell, L.O. Control of presynaptic function by a persistent Na(+) current. *Neuron* **60**, 975–979 (2008).
42. Hori, T. & Takahashi, T. Mechanisms underlying short-term modulation of transmitter release by presynaptic depolarization. *J. Physiol. (Lond.)* **587**, 2987–3000 (2009).
43. Awatramani, G.B., Price, G.D. & Trussell, L.O. Modulation of transmitter release by presynaptic resting potential and background calcium levels. *Neuron* **48**, 109–121 (2005).
44. Timmerman, W. & Westerink, B.H. Brain microdialysis of GABA and glutamate: what does it signify? *Synapse* **27**, 242–261 (1997).
45. Bianchi, L. *et al.* Investigation on acetylcholine, aspartate, glutamate and GABA extracellular levels from ventral hippocampus during repeated exploratory activity in the rat. *Neurochem. Res.* **28**, 565–573 (2003).
46. Maguire, J.L., Stell, B.M., Rafizadeh, M. & Mody, I. Ovarian cycle-linked changes in GABA(A) receptors mediating tonic inhibition alter seizure susceptibility and anxiety. *Nat. Neurosci.* **8**, 797–804 (2005).
47. Coulter, D.A. & Carlson, G.C. Functional regulation of the dentate gyrus by GABA-mediated inhibition. *Prog. Brain Res.* **163**, 235–243 (2007).
48. Wei, W., Faria, L.C. & Mody, I. Low ethanol concentrations selectively augment the tonic inhibition mediated by delta subunit-containing GABA<sub>A</sub> receptors in hippocampal neurons. *J. Neurosci.* **24**, 8379–8382 (2004).



## ONLINE METHODS

**Tissue preparation.** All procedures conformed to the Animals (Scientific procedures) Act 1986. Transverse hippocampal slices were prepared from 3–4-week-old Sprague Dawley rats using slightly different methods for the different experiments. For antidromic current threshold experiments (**Supplementary Fig. 1**) and for orthodromic transmission experiments (**Fig. 5**), both hippocampi were removed from the brain and placed in a block of agar before slicing (Leica VT1200S) in ice-cold sucrose-based solution containing 75 mM sucrose, 10 mM glucose, 87 mM NaCl, 2.5 mM KCl, 1.25 mM  $\text{NaH}_2\text{PO}_4$ , 7 mM  $\text{MgCl}_2$ , 0.5 mM  $\text{CaCl}_2$  and 25 mM  $\text{NaHCO}_3$  (bubbled with 95%  $\text{O}_2$  and 5%  $\text{CO}_2$ ). Slices (250–300  $\mu\text{m}$  thick) were then stored in an interface chamber before use. For mossy fiber bouton recordings (**Figs. 2–4**), slices were cut through the entire brain glued on the vibratome stage<sup>16,17</sup>. The slicing method for the  $\text{Ca}^{2+}$ -imaging experiments (**Fig. 5**), which allows optimal preservation of mossy fibers connected to their parent granule cells, was described previously<sup>21</sup>. Slices were transferred to the perfusion stage of an upright microscope (Olympus BX50WI or BX51WI) and recordings were obtained at 22–24 °C unless indicated. Drugs, chemicals and fluorophores were obtained from Tocris Cookson, Sigma or Invitrogen.

**Antidromic action current recordings.** Whole-cell pipettes used to record antidromic action currents contained 135 mM potassium gluconate, 8 mM NaCl, 10 mM HEPES, 2 mM MgATP, 0.3 mM  $\text{Na}_3\text{GTP}$  and 0.2 mM EGTA (pH 7.2, osmolarity 295 mOsm). Extracellular stimuli were delivered via a bipolar electrode positioned in stratum lucidum, between 500 and 1,500  $\mu\text{m}$  from the granule cell (stimulus duration, 500  $\mu\text{s}$ ; interval, 10 s), and granule cells were clamped at –60 mV. Recordings were only accepted if the action current latency was >2 ms. The access and input resistances were monitored using a –5-mV voltage step command. The access resistance was <20 M $\Omega$  and results were discarded if it changed by more than 20%. Junction potentials were not corrected. The stimulus was cycled through a saw-tooth intensity pattern ranging from 100% failures to 100% success for evoking an action current. THDOC and GBX application was associated with a small decrease in somatic holding current (THDOC,  $18.7 \pm 5.8$  pA,  $n = 8$ ; GBX,  $61.1 \pm 19.3$  pA,  $n = 4$ ), consistent with tonically active somatodendritic GABA<sub>A</sub> receptors. For perforated-patch recordings, gramicidin was dissolved in dimethylsulfoxide. This stock solution was mixed with potassium gluconate-based internal pipette solution just before use to a final concentration of 100  $\mu\text{g ml}^{-1}$ . An access resistance of 40–60 M $\Omega$  was obtained 20–40 min after formation of a gigaseal.

Currents were acquired with an Axopatch 1D amplifier (Axon Instruments) and records were filtered at 2 kHz, digitized at 10–20 kHz and stored on a personal computer. Action current success rates were calculated from 10–15 trials per plotted point. The stimulus intensity required to obtain a 50% success rate,  $\text{stim}_{50}$ , was obtained by fitting the relationship of the action current success rate  $A$  to stimulus intensity  $s$  with a logistic equation,  $A = 1/[1 + (\text{stim}_{50}/s)^h]$ , with  $h$  being analogous to a Hill coefficient. Because the minimal and maximal stimulus intensities and increment amplitudes were set empirically for each cell, these input-output curves were only used to obtain a qualitative insight into changes in axon excitability.

**Mossy fiber bouton recordings.** The perfusion solution for mossy fiber bouton recordings contained 125 mM NaCl, 2.5 mM KCl, 1.25 mM  $\text{NaH}_2\text{PO}_4$ , 1 mM  $\text{MgCl}_2$ , 2 mM  $\text{CaCl}_2$ , 25 mM  $\text{NaHCO}_3$  and 11 mM glucose. For single-channel recordings, pipettes were fabricated from thick-walled borosilicate glass (outer diameter, 2 mm; inner diameter, 0.6 mm), pulled and fire polished to obtain a final resistance of 8–15 M $\Omega$ . Pipettes used for bouton-attached or whole-bouton recordings were pulled from standard tubing (outer diameter, 1.5 mm; inner diameter, 0.75). Mossy fiber boutons were visualized in stratum lucidum using infrared differential interference contrast optics as small spherical structures (4–6  $\mu\text{m}$ ). A differential interference contrast image of the recorded mossy fiber bouton was taken routinely before each recording attempt. We confirmed that boutons recorded in cell-attached mode were able to follow extracellular stimulation at 200 Hz. The series resistance was typically 15–35 M $\Omega$ . For high  $[\text{Cl}^-]_i$  whole-bouton recordings in current clamp, the pipette solution contained 155 mM KCl, 10 mM HEPES, 2 mM  $\text{Na}_2\text{ATP}$ , 0.3 mM  $\text{Na}_3\text{GTP}$  and 0.2 mM EGTA. For normal  $[\text{Cl}^-]_i$  recordings, the KCl concentration was reduced to 20 mM and 135 mM  $\text{KMeSO}_4$  was added. Whole-bouton voltage-clamp recordings were performed with a pipette solution containing 145 mM CsCl, 8 mM NaCl, 2 mM  $\text{MgCl}_2$ ,

10 mM HEPES, 2 mM  $\text{Na}_2\text{ATP}$ , 0.5 mM  $\text{Na}_3\text{GTP}$  and 2 mM EGTA. In some experiments, the pipette solution also contained 0.4% biocytin (wt/vol) for *post hoc* visualization with confocal imaging. In five of seven slices in which visualization was attempted, the basic anatomy of a mossy fiber bouton and parent axon could be recovered, confirming that the recordings originated from presynaptic elements (**Supplementary Fig. 2**). Local pressure application of THDOC (50 nM in control perfusion solution) or gabazine (10  $\mu\text{M}$ ) was delivered via a patch pipette connected to a Picospritzer (General Valve, 5–50 ms, 5–20 psi).

Outside-out patches from mossy fiber boutons were obtained with a symmetric  $\text{Cl}^-$ -based internal pipette solution containing 145 mM CsCl, 8 mM NaCl, 2 mM  $\text{MgCl}_2$ , 10 mM HEPES, 2 mM  $\text{Na}_2\text{ATP}$ , 0.5 mM  $\text{Na}_3\text{GTP}$ , 2 mM EGTA and 5 mM sodium phosphocreatine. Patches were pulled from mossy fiber boutons after checking high-frequency spike fidelity in response to five extracellular stimuli at 200 Hz in cell-attached mode (**Supplementary Fig. 2**) and held in voltage-clamp at –60 mV. Channel behavior was measured by applying voltage pulses (–120 mV to +40 mV, step 20 mV). Patches with spontaneous channel openings in the absence of muscimol or patches exhibiting more than one modal conductance level were not retained for further analysis. Signals were recorded with an Axopatch 200A sampled at 20 kHz, low-pass filtered at 2 kHz (–3 dB, 8-pole Bessel) and stored on a personal computer for off-line analysis with PClamp 9.0 (Axon Instruments). Analysis of single-channel activity was performed on 20–40 s recording epochs at each holding potential. Single-channel open period duration and amplitude distributions were fitted with a sum of multiple Gaussian components using Levenberg-Marquardt least-square minimization (Microcal Origin 6.0).

To estimate the membrane potential of unperturbed mossy fiber boutons, we used terminal-attached recordings as described for cell-attached recordings<sup>19</sup>. The pipette solution contained 155 mM KCl, 10 mM EGTA, 8 mM NaCl, 4 mM  $\text{MgCl}_2$ , 0.3 mM MgATP, 0.3 mM  $\text{Na}_3\text{GTP}$ , 10 mM HEPES and 10 mM sodium phosphocreatine. Patches were held in tight seal configuration at –60 mV (pipette potential,  $V_p = +60$  mV) and ramp depolarization applied from –100 mV to +200 mV (3 mV  $\text{ms}^{-1}$ ) to elicit  $\text{K}^+$  currents. The reversal potential for  $\text{K}^+$ -mediated currents was calculated by fitting a straight line to the average macroscopic current amplitude as a function of potential; this typically corresponded to the interval between 1–5 ms after ramp onset. The intercept between the linear fit and the average of ten successive current traces was used to determine the reversal of  $\text{K}^+$  current, and therefore the  $E_m$  of individual terminals. The seal conductance is irrelevant in these measurements, as it affects the holding current value recorded at each potential, but not the voltage for which reversal occurs<sup>18,19</sup>.

For visualization of biocytin-filled boutons, slices were fixed overnight in 4% paraformaldehyde (wt/vol) at 4 °C. After permeabilization in 0.1% Triton X-100 (wt/vol), slices were incubated in 0.1% streptavidin–Alexa 488 conjugate (wt/vol), mounted in DABCO anti-fading medium and imaged with a Zeiss LSM 510 meta-confocal microscope.

**Postsynaptic recordings.** Recordings from CA3 pyramidal neurons were obtained with one of two pipette solutions. For the experiments in **Figure 6**, the solution contained 120 mM CsF, 1 mM DIDS, 10 mM HEPES, 2 mM  $\text{MgCl}_2$ , 2 mM MgATP, 0.3 mM  $\text{Na}_3\text{GTP}$ , 0.2 mM EGTA and 5 mM QX314 Br. For the experiments in **Figure 7**, 112 mM cesium gluconate and 8 mM NaCl were substituted for CsF, DIDS was omitted, the EGTA concentration was increased to 5 mM and the cell was held at –60 mV, close to the estimated reversal potential for GABA<sub>A</sub> receptors. The pressure-application pipette was positioned 50–200  $\mu\text{m}$  from the apical dendrite of the recorded CA3 pyramidal neuron, allowing for selective manipulation of presynaptic GABA<sub>A</sub> receptors by puffing THDOC (50 nM; **Fig. 6**) or gabazine (10  $\mu\text{M}$ ; **Figs. 6** and **7**). GABA<sub>B</sub> and NMDA receptors were blocked throughout. EPSCs were evoked via a stimulus electrode positioned in the dentate granule cell layer. Mossy fiber EPSCs were only accepted if they exhibited marked facilitation when the stimulation frequency was switched from 0.05 to 1 Hz and were depressed by DCG-IV (1  $\mu\text{M}$ ) at the end of the experiment. Stabilization of EPSC amplitude was usually observed within 15–20 min of break-in. LTP was induced with three 100-Hz trains, lasting 1 s, with a 10-s interval between trains. Gabazine was pressure applied before each train, with a 50-ms interval between the end of the puff and the start of the train.

**$\text{Ca}^{2+}$  imaging.** For  $\text{Ca}^{2+}$ -imaging experiments, we used a Radiance 2000 confocal microscope (BioRad, Zeiss) that was optically linked to a MaiTai fs pulsed infrared

laser (SpectraPhysics) and integrated with patch-clamp electrophysiology. Granule cells or CA3 pyramidal neurons were recorded in whole-cell mode with a pipette solution containing 150 mM KMeSO<sub>4</sub>, 5 mM KCl, 2 mM MgCl<sub>2</sub>, 10 mM HEPES, 10 mM sodium phosphocreatine, 4 mM Na<sub>2</sub>ATP, 0.4 mM Na<sub>3</sub>GTP, 20–40 μM Alexa Fluor 594 and 200 μM Fluo-4. Both fluorophores were excited at  $\lambda_{\text{ex}} = 800$  nm. Giant boutons synapsing on CA3 pyramidal cells were traced 400–800 μm from the soma and recordings started at least 1 h after obtaining a whole-cell configuration, at which point dye concentrations have equilibrated<sup>21</sup>. For Schaffer collateral recordings, boutons (200–400 μm from the soma, in the CA3 region) were either selected on the main axon or on side branches (**Supplementary Fig. 6**) and the results were pooled together because no differences were found in their response to GABA<sub>A</sub> receptor manipulation.

Fluorescence line scans (500 or 1,000 ms long) were recorded at 500 Hz, with an inter-sweep interval of either 30 s or 1 min, and analyzed off-line. Action potentials were evoked using 1-ms depolarizing voltage command pulses delivered via the somatic pipette. To minimize the effect of focus drift, optical noise, extracellular fluorescence changes or fluctuations in resting Ca<sup>2+</sup>, we calculated the amplitude of the Ca<sup>2+</sup>-dependent fluorescence transient as  $\Delta F/R = (F_{\text{post}} - F_{\text{o}})/R$ ;  $F_{\text{o}}$  and  $F_{\text{post}}$  denote the fluorescence intensity in the green Fluo-4 channel averaged over the visible bouton during 100-ms windows before and after the spike, respectively, and  $R$  denotes the Ca<sup>2+</sup>-independent fluorescence intensity

in the red Alexa channel sampled in the same ROI. In these imaging conditions, Fluo-4 is far from saturation and can provide an accurate gauge of action potential-evoked presynaptic Ca<sup>2+</sup> concentration changes<sup>21–23</sup>. Image analysis was performed on stacks of stored images using NIH Image macros (<http://rsb.info.nih.gov/nih-image/>). False color tables and averaged images were used for illustration purposes, but the quantitative analyses always applied to the original gray level images of each individual line scan.

For epifluorescence wide-field imaging of HFS-evoked Ca<sup>2+</sup> transients, 5–15 μl of 30–40 μM Fura2-AM was injected close to the site of stimulation in the dentate hilus. Field excitatory postsynaptic potentials were initially recorded to verify that the stimulation electrode activated mossy fibers, and ionotropic glutamate receptors were blocked with NBQX and AP5 before fluorescence image acquisition. Fura2 was alternately excited at 340 and 380 nm for 200 ms (25 image pairs) with a Polychrome IV monochromator under the control of TillVision software (Till Photonics) and images were acquired with an Imago CCD camera. Gabazine (10 μM) or zolpidem (20 μM) was pressure applied (5–10 psi) for 250 ms, terminating 50 ms before HFS. Three successive HFS trains were applied with or without drug application, with 4-min intervals. Pressure application of vehicle (ACSF) was without effect.

**Statistics.** Statistical comparisons were made using Student's paired *t* test or the Mann-Whitney *U*-test for unpaired data (**Fig. 2b**). Data are reported as mean ± s.e.m.